Report

Cell Reports

Dorsal raphe serotonergic neurons preferentially reactivate dorsal dentate gyrus cell ensembles associated with positive experience

Graphical abstract

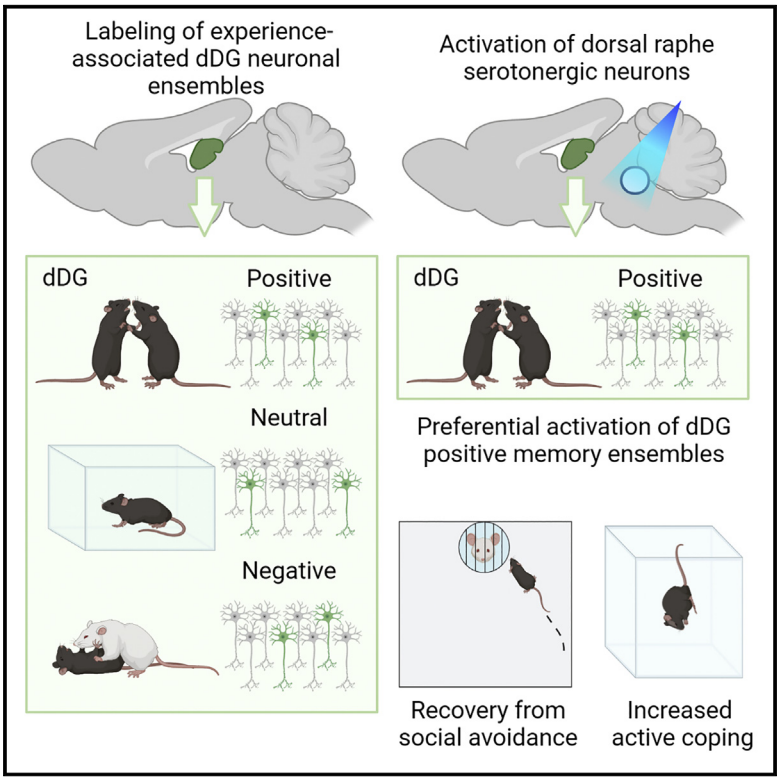

Highlights

- Activation of dorsal raphe serotonin neurons produces an antidepressant-like effect
- Activation of dDG-positive memory ensembles produces an antidepressant-like effect
- Dorsal raphe serotonin neurons preferentially activate dDG-positive memory ensembles
- Dopamine mediates the positive ensemble reactivation and active coping behaviors

Authors

Yuma Nagai, Yuri Kisaka, Kento Nomura, ..., Takanobu Nakazawa, Hitoshi Hashimoto, Shuji Kaneko

Correspondence

nagayasu@pharm.kyoto-u.ac.jp (K.N.), skaneko@pharm.kyoto-u.ac.jp (S.K.)

In brief

Serotonergic neurons are central to major depressive disorder pathophysiology and treatment. Repeatedly recalling positive episodes is effective for major depressive disorder. Nagai et al. show that dorsal raphe serotonergic neurons preferentially activate positive-experience-associated neuronal ensembles in the dorsal dentate gyrus, a key brain region in memory processing.

Nagai et al., 2023, Cell Reports *42*, 112149
March 28, 2023
https://doi.org/10.1016/j.celrep.2023.112149

CellPress

Cell Reports

CellPress
OPEN ACCESS

Report

Dorsal raphe serotonergic neurons preferentially reactivate dorsal dentate gyrus cell ensembles associated with positive experience

Yuma Nagai,[1] Yuri Kisaka,[1] Kento Nomura,[1] Naoya Nishitani,[2] Chihiro Andoh,[1] Masashi Koda,[1] Hiroyuki Kawai,[1] Kaoru Seiriki,[3] Kazuki Nagayasu,[1,9,*] Atsushi Kasai,[3] Hisashi Shirakawa,[1] Takanobu Nakazawa,[4] Hitoshi Hashimoto,[3,5,6,7,8] and Shuji Kaneko[1,*]

[1]Department of Molecular Pharmacology, Graduate School of Pharmaceutical Sciences, Kyoto University, 46-29 Yoshida-Shimoadachi-cho, Sakyo-ku, Kyoto 606-8501, Japan

[2]Laboratory of Molecular Pharmacology, Institute of Medical, Pharmaceutical and Health Sciences, Kanazawa University, Kanazawa 920-1192, Japan

[3]Laboratory of Molecular Neuropharmacology, Graduate School of Pharmaceutical Sciences, Osaka University, 1-6 Yamadaoka, Suita, Osaka 565-0871, Japan

[4]Laboratory of Molecular Biology, Department of Bioscience, Graduate School of Life Sciences, Tokyo University of Agriculture, 1-1-1 Sakuragaoka, Setagaya-ku, Tokyo 156-8502, Japan

[5]Molecular Research Center for Children's Mental Development, United Graduate School of Child Development, Osaka University, Kanazawa University, Hamamatsu University School of Medicine, Chiba University and University of Fukui, 1-6 Yamadaoka, Suita, Osaka 565-0871, Japan

[6]Division of Bioscience, Institute for Datability Science, Osaka University, 1-1 Yamadaoka, Suita, Osaka 565-0871, Japan

[7]Transdimensional Life Imaging Division, Institute for Open and Transdisciplinary Research Initiatives, Osaka University, 2-1 Yamadaoka, Suita, Osaka 565-0871, Japan

[8]Department of Molecular Pharmaceutical Science, Graduate School of Medicine, Osaka University, 2-2 Yamadaoka, Suita, Osaka 565-0871, Japan

[9]Lead contact

*Correspondence: nagayasu@pharm.kyoto-u.ac.jp (K.N.), skaneko@pharm.kyoto-u.ac.jp (S.K.)

https://doi.org/10.1016/j.celrep.2023.112149

SUMMARY

Major depressive disorder (MDD) is among the most common mental illnesses. Serotonergic (5-HT) neurons are central to the pathophysiology and treatment of MDD. Repeatedly recalling positive episodes is effective for MDD. Stimulating 5-HT neurons of the dorsal raphe nucleus (DRN) or neuronal ensembles in the dorsal dentate gyrus (dDG) associated with positive memories reverses the stress-induced behavioral abnormalities. Despite this phenotypic similarity, their causal relationship is unclear. This study revealed that the DRN 5-HT neurons activate dDG neurons; surprisingly, this activation was specifically observed in positive memory ensembles rather than neutral or negative ensembles. Furthermore, we revealed that dopaminergic signaling induced by activation of DRN 5-HT neurons projecting to the ventral tegmental area mediates an increase in active coping behavior and positive dDG ensemble reactivation. Our study identifies a role of DRN 5-HT neurons as specific reactivators of positive memories and provides insights into how serotonin elicits antidepressive effects.

INTRODUCTION

Major depressive disorder (MDD), characterized by heterogeneous symptoms including depressed mood and anhedonia, is among the most common mental illnesses worldwide.[1,2] Serotonergic neurons (5-HT neurons) are central to MDD pathophysiology and treatment.[3–8] Accordingly, selective serotonin reuptake inhibitors (SSRIs), which enhance serotonergic neurotransmission, are first-line MDD treatments.[9–13] Furthermore, 5-HT neuron activation in the dorsal raphe nucleus (DRN), the largest 5-HT nucleus in the brain, elicits antidepressant-like effects[14–16]; these effects disappear rapidly after the termination of optogenetic stimulation.[16] Zou et al. showed that chronic stimulation of the DRN 5-HT neurons projecting to the ventral tegmental area (VTA) reversed the social interaction deficit induced by chronic social defeat stress (CSDS), and the effect continued even after the termination of optogenetic stimulation.[17] However, the underlying mechanisms are unclear.

Clinical evidence shows that memory recall is important in MDD pathophysiology and treatment. Patients with MDD exhibit significant difficulties in recalling positive memories and tend to recall negative memories.[18–21] A meta-analysis demonstrated that repeatedly recalling positive episodes improved MDD symptoms.[22] Memory is retrieved when neuronal ensembles

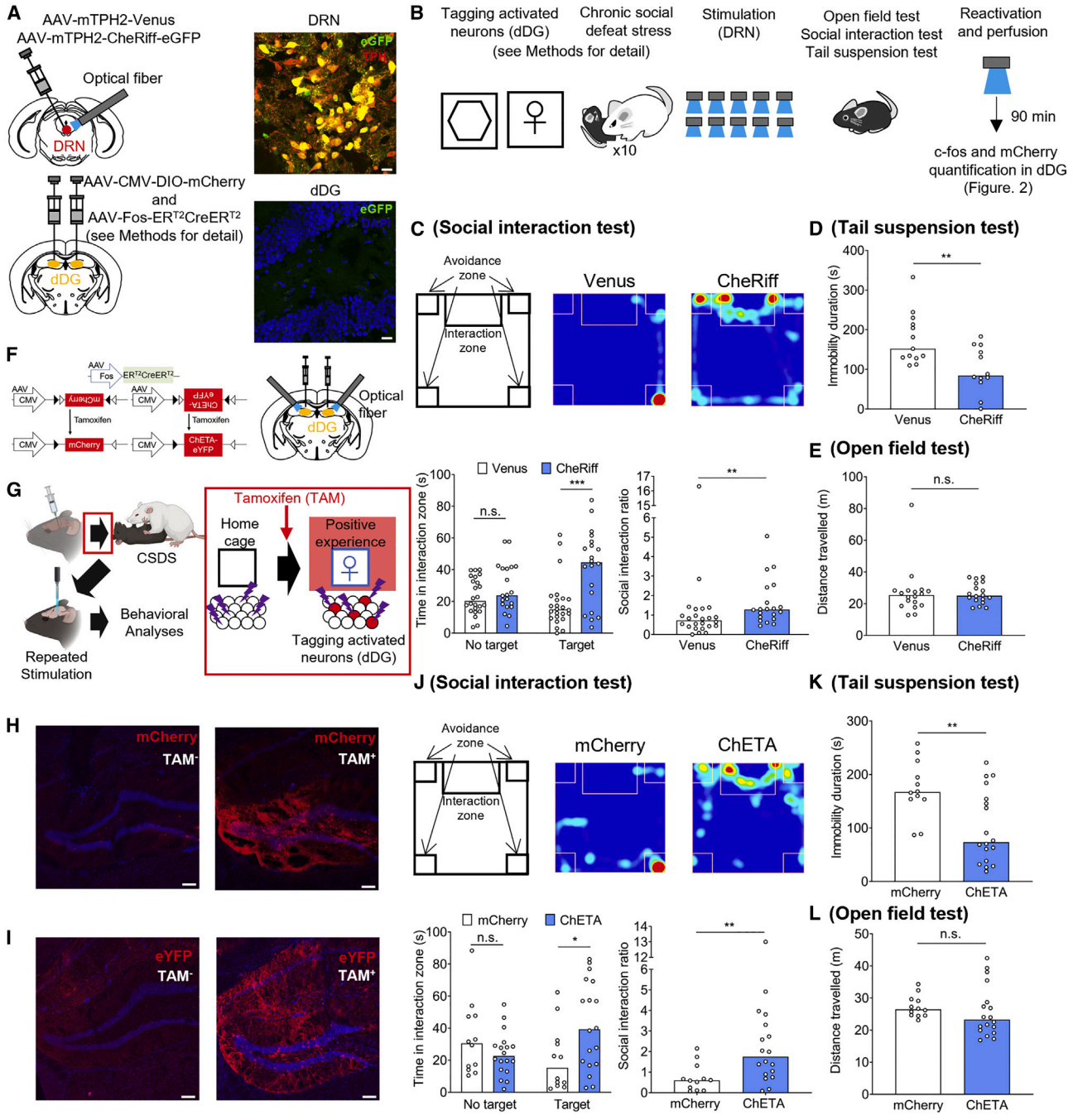

Figure 1. Repeated activation of DRN 5-HT neurons and positive dDG ensembles reverses CSDS-induced depression-like behavioral changes

(A) Left: Schematic illustration of experiment. Right: Representative image of eGFP (green), TPH (red), and nuclei (DAPI, blue). Scale bar, 20 μm.

(B) Experimental design (see STAR Methods for details). ♀ and hexagons: contact with a female mouse and exploration in a novel cage, respectively.

(C) Top: Schematic illustration of the chamber and representative heat maps (target session). Bottom: Time spent in the interaction zone. Social interaction ratio: the ratio of time spent in the interaction zone during a target and no-target session; n = 24 (Venus) and 20 (CheRiff) mice.

(D) Immobility duration in the tail suspension test; n = 13 (Venus) and 12 (CheRiff) mice.

(E) Locomotor activity in the open field test; n = 18 (Venus) and 18 (CheRiff) mice.

(F) Left: Schematic diagram of tamoxifen (TAM)-induced flip-excision. Right: Schematic illustration of experiment.

(G) Experimental design. Created with BioRender.com.

(H and I) TAM injection induced robust transgene expression in the dDG. Scale bar, 100 μm.

(legend continued on next page)

(especially in the hippocampus) that were activated during a particular experience are reactivated by the subsequent presentation of similar conditions.[23–25] Some studies have suggested a link between memory-related neuronal ensembles in the hippocampus and the pathogenesis and improvement of a depression-like state in rodents.[26,27] Ramirez et al. demonstrated that optogenetic reactivation of the dorsal dentate gyrus (dDG) neuronal ensembles associated with a naturally rewarding (positive) experience induces an antidepressant-like effect.[26] Interestingly, this antidepressant-like effect disappeared 1 day after reactivation, whereas a 5-day regimen of repeated reactivation persistently improved chronic restraint stress-induced depression-like behavior.[26]

Collectively, these studies suggest that acute activation of DRN 5-HT neurons and dDG neuronal ensembles associated with positive experience can transiently improve depression-like behavior, whereas chronic stimulation leads to persistent recovery. Importantly, pharmacological enhancement of 5-HT neuronal transmission and repeated recall of positive episodes are commonly used in MDD treatment. Despite their phenotypic similarity, it is unclear whether and how these two neuronal populations are causally linked.

In this study, we showed that activation of VTA-projecting DRN 5-HT neuron preferentially reactivates the positive-experience-associated dDG neuronal ensemble via dopaminergic (DA) signaling. Lack of sociality and increased passive coping to inescapable stress induced by CSDS were reversed by repeated stimulation of DRN 5-HT neurons, VTA-projecting DRN 5-HT (5-HT$^{DRN\rightarrow VTA}$) neurons, or dDG neuronal ensembles activated during a naturally rewarding experience. Histological analysis revealed that DRN 5-HT or 5-HT$^{DRN\rightarrow VTA}$ neuron activation increases the activity of dDG neurons; surprisingly, this activity increase was specifically observed in positive memory ensembles rather than neutral or negative ensembles. Dopamine receptor antagonists blunted the increased active coping behavior and positive memory ensemble reactivation in the dDG but did not affect the recovery from lack of sociality. Our study, for the first time, identifies a role of DRN 5-HT neurons as a specific reactivator of positive memories and provides insights into how serotonin elicits antidepressive effects.

RESULTS

Effects of repeated activation of the DRN 5-HT neurons or dDG neuronal ensembles associated with positive experience on CSDS-induced aberrant behaviors

We studied how repeated DRN 5-HT neuron activation affects the lack of sociality and increases passive coping behavior after CSDS[28] (Figures 1A–1E, S1A, and S1C–S1F). Adeno-associated virus (AAV) vectors bearing the excitatory optogenetic actuator CheRiff under the mouse tryptophan hydroxylase 2 (TPH2) promoter were injected into the DRN[29,30] (Figures S1C–S1E). After CSDS, mice were subjected to optogenetic activation for 5 days (5 min/session, two sessions/day), followed by an open field, social interaction, and tail suspension test (OFT, SIT, and TST, respectively) (Figures 1C–1E). As previously reported,[17] CheRiff-expressing mice spent significantly more time in the interaction zone and had a higher social interaction ratio than the Venus control (Figure 1C). Moreover, the immobility duration of CheRiff-expressing mice in the TST, used as a proxy of a depression-like state, was significantly shorter than that of Venus-expressing mice (Figure 1D). In the OFT, we observed no significant difference in travel distance between the groups (Figure 1E). Thus, repeated DRN 5-HT neuron activation reverses the lack of social reward and passive coping behaviors after CSDS.

Ramirez et al. showed that repeated activation of a positive memory engram in the dDG elicits antidepressant-like effects in the TST after chronic restraint stress.[26] To assess the same effect following CSDS, we repeatedly activated positive-experience-associated dDG neuronal ensembles and assessed CSDS-induced depression-like behaviors (Figures 1F–1L, S1B, and S1G). Using a tamoxifen (TAM)-dependent Cre recombinase activation system (ER^{T2}CreER^{T2}), we tagged the neurons that were active during a particular experience.[31] We injected an AAV expressing either the excitatory optogenetic actuator ChETA,[16,32] or mCherry in a Cre-dependent manner into the dDG along with AAV-Fos-ER^{T2}CreER^{T2}. Four weeks after AAV injection, we implanted optical fibers into the dDG. Subsequently, TAM (3 mg/mouse, intraperitoneal [i.p.] administration) was injected 6 h before exposure to a female mouse, a representative naturally rewarding (positive) experience, to label dDG neuronal ensembles (dDG-positive ensembles) (Figures 1F and 1G). Histological analysis confirmed transgene expression in the dDG upon TAM injection (Figures 1H and 1I). After CSDS, mice were subjected to a 5-day regimen of dDG activation (15 min/session, two sessions/day). Next, mice underwent the OFT, SIT, and TST (Figures 1J–1L). In the SIT, ChETA-expressing mice spent more time in the interaction zone than mCherry mice did, resulting in a higher social interaction ratio (Figure 1J). In the TST, the immobility duration of the ChETA group was significantly shorter than that of the mCherry group (Figure 1K). In the OFT, we observed no significant difference in locomotor activity between the groups (Figure 1L). These results indicate that repeated reactivation of a positive ensemble in the dDG reverses CSDS-induced depression-like behavior.

DRN 5-HT neuron activation elicits preferential reactivation of positive ensembles in the dDG

Although the behavioral consequences of DRN 5-HT neuron and positive dDG ensemble activation are phenotypically similar, their causal relationships are unclear. Thus, we examined whether DRN 5-HT neurons and positive dDG ensembles activate each other (Figures 2 and S2). We injected AAV-Fos-ER^{T2}CreER^{T2} and AAV-CMV-DIO-mCherry into the dDG and concurrently injected AAV-mTPH2-Venus or AAV-mTPH2-CheRiff-eGFP injection into

(J) Top: Schematic illustration of the chamber and representative heat maps (target session). Bottom: Time spent in the interaction zone. Social interaction ratio: same as in (C); n = 12 (mCherry) and 18 (ChETA) mice.
(K) Immobility duration in the tail suspension test; n = 12 (mCherry) and 18 (ChETA) mice.
(L) Locomotor activity in the open field test; n = 12 (mCherry) and 18 (ChETA) mice. *p < 0.05, **p < 0.01, ***p < 0.001. See also Figure S1.

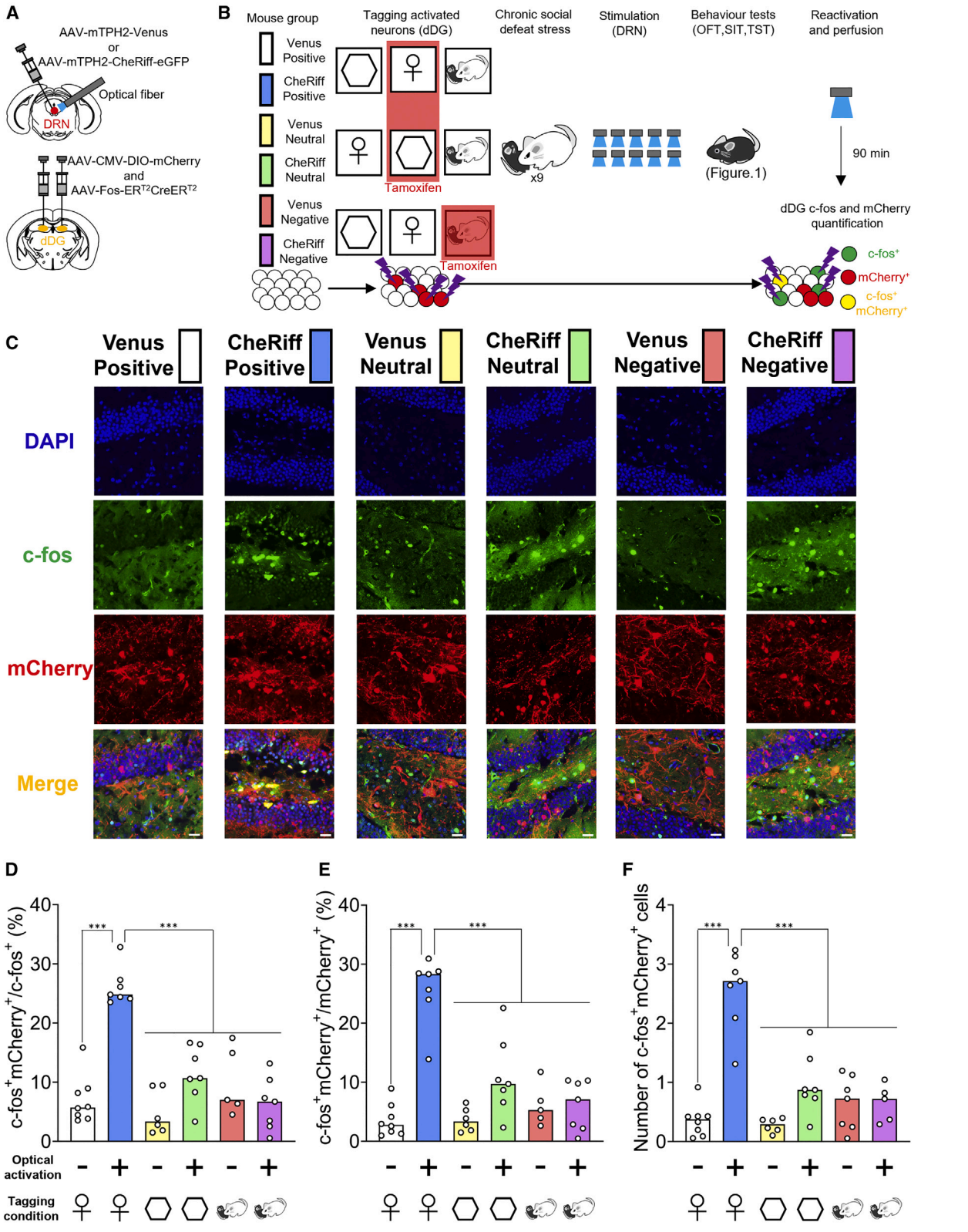

(legend on next page)

the DRN. An optical fiber was then implanted in the DRN (Figure 2A). At 6 h after TAM injection, mice experienced cohabitation with a female mouse (positive experience), the exploration of a new cage (neutral experience), or a single social defeat session (negative experience). The dDG neuronal ensembles associated with each experience were labeled with mCherry (positive, neutral, and negative ensembles).[26,27] After CSDS, repeated DRN 5-HT neuron activation, and behavioral analyses (shown in Figures 1C–1E; see STAR Methods for details), we performed further DRN 5-HT neuron stimulation. The mice were sacrificed 90 min later and subjected to immunohistochemical analysis. Mice expressing CheRiff in the DRN and mCherry in positive dDG ensembles (CheRiff-positive) showed a significantly higher c-fos-mCherry colocalization rate and c-fos$^+$mCherry$^+$ cell counts in the dDG than the other groups (Figures 2C–2F and S2A). Conversely, mCherry$^+$ cell counts were similar in all groups (Figure S2B), whereas c-fos$^+$ cell counts increased significantly in CheRiff-expressing mice irrespective of their experience (Figure S2C). These results suggest that DRN 5-HT neuron activation preferentially reactivates the positive dDG ensembles.

Naturally rewarding experiences activate DRN 5-HT neurons.[33] However, it is unclear whether reactivation of positive dDG ensembles is sufficient to activate DRN 5-HT neurons. Therefore, we investigated c-fos expression in the DRN after reactivation of positive dDG ensembles (Figures S2D–S2I). We injected AAV-Fos-ER^{T2}CreER^{T2} and AAV-CMV-DIO-mCherry or AAV-CMV-DIO-ChETA-eYFP into the dDG and implanted an optical fiber in the dDG. We applied CSDS after tagging the positive dDG ensemble using TAM. The mice were then subjected to optogenetic activation and behavioral analyses and sacrificed after positive dDG ensemble reactivation, and we analyzed c-fos expression in the DRN (Figures S2F–S2I). The proportion of c-fos$^+$ cells among all DAPI$^+$ cells (c-fos$^+$/DAPI$^+$; Figure S2G), that of c-fos$^+$TPH2$^+$ cells among all TPH2$^+$ cells (c-fos$^+$TPH2$^+$/TPH2$^+$; Figure S2H), and c-fos$^+$TPH2$^+$ cell counts (Figure S2I) in the DRN did not differ significantly between the groups, whereas optogenetic DRN 5-HT neuron stimulation led to a robust increase in c-fos expression in these neurons (Figures S1C–S1E).

5-HT$^{DRN\rightarrow VTA}$ neuron activation elicits antidepressant-like effects in a CSDS paradigm, and dDG neuronal ensemble reactivation is preferentially associated with positive experience

We investigated how 5-HT$^{DRN\rightarrow VTA}$ neuron activation affects CSDS-induced depression-like behaviors and dDG neuronal ensemble reactivation. We injected AAV-mTPH2-Venus or AAV-mTPH2-CheRiff-eGFP into the DRN and AAV-Fos-ER^{T2}-CreER^{T2} and AAV-CMV-DIO-mCherry into the dDG. We implanted optical fibers into the VTA (Figure 3A). We observed strong GFP expression in the VTA, indicating sufficient CheRiff expression in the VTA (Figure 3B). After tagging of dDG ensembles, mice were subjected to CSDS, 5-HT$^{DRN\rightarrow VTA}$ neuron activation for 5 days, and behavioral analyses (Figures 3C–3F and S3A). In the SIT, the CheRiff group spent significantly more time in the interaction zone and displayed a higher social interaction ratio than the Venus group (Figure 3D). In the TST, the immobility duration of the CheRiff group was significantly shorter than that of the Venus group (Figure 3E). However, we observed no significant difference in locomotor activity between the groups in the OFT (Figure 3F). After behavioral analyses, we further stimulated the 5-HT$^{DRN\rightarrow VTA}$ neurons and then sacrificed the mice. We observed significantly higher c-fos-mCherry colocalization rates and c-fos$^+$mCherry$^+$ cell counts in the CheRiff-positive group than in the other groups (Figures 3G–3I and S3B–S3E). Conversely, mCherry$^+$ cell counts were similar in all six groups (Figure S3C), whereas c-fos$^+$ cell numbers increased significantly in the CheRiff group irrespective of the experience (Figure S3D). These results indicate that 5-HT$^{DRN\rightarrow VTA}$ neuron reactivates positive dDG ensembles and elicits antidepressant-like effects.

DA signaling mediates an increase in active coping behavior and the preferential reactivation of positive dDG ensembles by 5-HT$^{DRN\rightarrow VTA}$

Activation of the DRN 5-HT axon terminals in the VTA causes DA neuron excitation.[34] Consistent with this finding, optogenetic 5-HT$^{DRN\rightarrow VTA}$ neuron stimulation increased the number of c-fos and tyrosine hydroxylase double-positive cell numbers in the VTA (Figures S3F–S3J). We tested whether DA signaling was necessary for the antidepressant-like effects and preferential reactivation of the positive-experience-associated dDG neuronal ensembles by 5-HT$^{DRN\rightarrow VTA}$ neurons (Figures 4A, 4B, and S4A). To inhibit DA signaling, we administered a combination of SCH23390 (0.1 mg/kg, i.p.), a D_1 receptor antagonist, and raclopride (2 mg/kg, i.p.), a D_2 receptor antagonist (D1+D2 group), 20 min before optogenetic stimulation. In the SIT, we observed no significant differences between the groups in the time spent in the interaction zone during a target session or the social interaction ratio (Figure 4C), indicating that DA signaling is not necessary for the social avoidance reduction elicited by 5-HT$^{DRN\rightarrow VTA}$ neuron activation. In the TST, the immobility duration in the D1+D2 group was significantly longer than that in the vehicle group (Figure 4D). However, there was no significant difference in locomotor activity in the OFT (Figure 4E). Finally, we investigated how D_1 and D_2 antagonists affect positive

Figure 2. DRN 5-HT neuron activation preferentially reactivates positive-experience-associated dDG neuronal ensembles

(A) Schematic illustration of experiment.

(B) Experimental design. ♀ and hexagons: contact with a female mouse and exploration in a novel cage, respectively. Red squares: tamoxifen administration. Neuronal ensembles associated with a positive, neutral, or negative experience were tagged using tamoxifen. Optogenetic stimulation was applied, and the mice were sacrificed for immunohistochemical analyses.

(C) Representative images for DAPI (blue), c-fos (optogenetically activated cells; green), and mCherry (tamoxifen-tagged neuronal ensembles; red) in the dDG; scale bars, 20 μm.

(D–F) Quantification of the c-fos$^+$mCherry$^+$-to-c-fos$^+$ (D) and -mCherry$^+$ (E) cell colocalization rates, and c-fos$^+$mCherry$^+$ cell numbers (F); n = 7 (CheRiff-Positive, CheRiff-Neutral, and CheRiff-Negative), 8 (Venus-Positive), 6 (Venus-Neutral), and 5 (Venus-Negative) mice. ***p < 0.001. See also Figure S2.

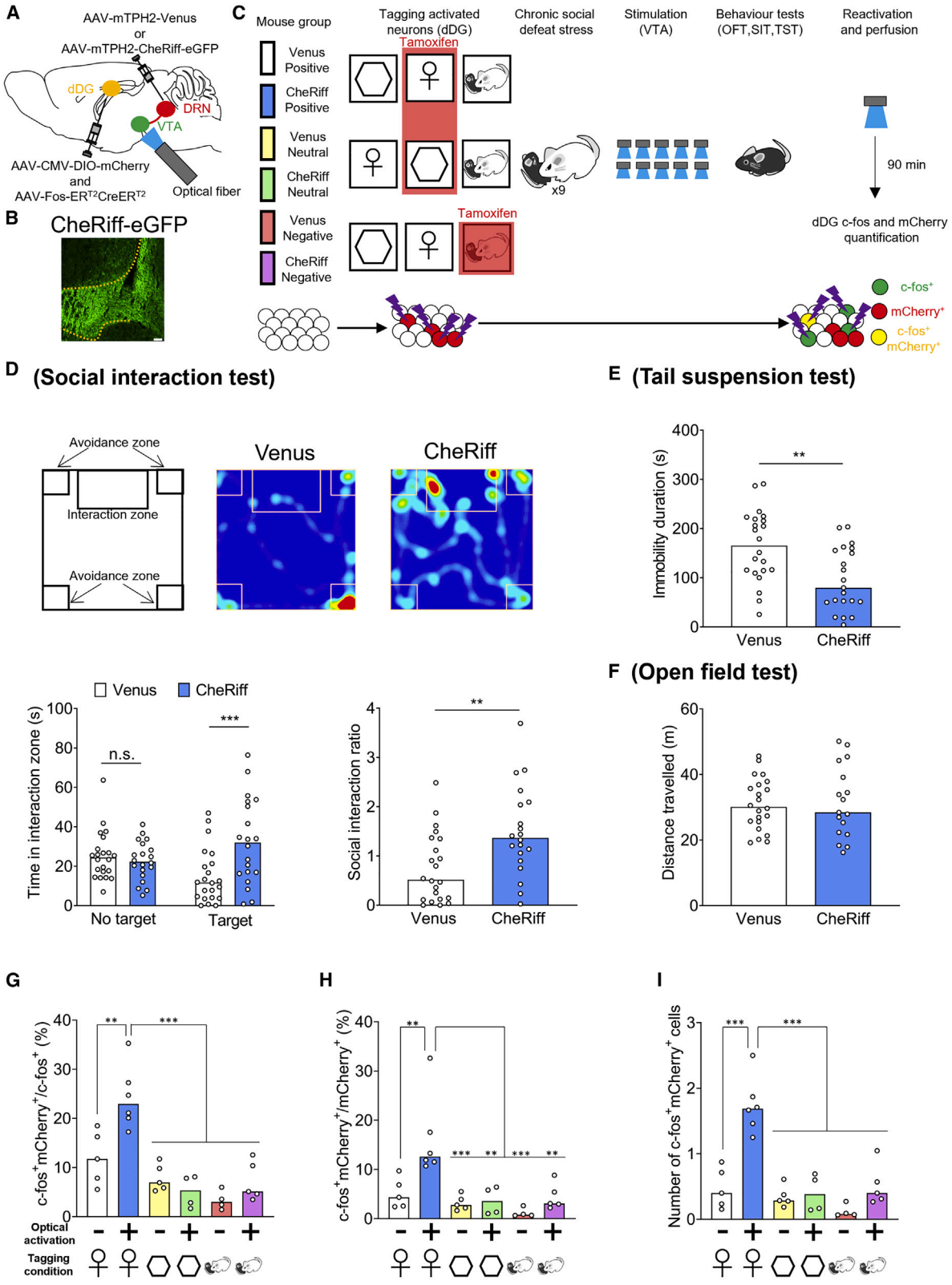

(legend on next page)

dDG ensemble reactivation. The c-fos-mCherry colocalization rate and c-fos$^+$mCherry$^+$ cell counts were significantly lower in the D1+D2 group than in the vehicle control (Figures 4F–4H and S4B). Conversely, c-fos$^+$ and mCherry$^+$ cell counts were similar between the groups (Figures S4C and S4D). No significant effect of D_1 and D_2 antagonist treatment was observed in CheRiff-expressing mice without photoactivation or in Venus-expressing mice with photoactivation (Figures S4F–S4H). These results indicate that DA signaling is necessary for the recovery of active coping with inescapable stress and reactivation of positive dDG ensembles elicited by activation of 5-HT$^{DRN\rightarrow VTA}$ neurons.

DISCUSSION

Although clinical evidence has demonstrated the therapeutic efficacy of SSRIs for MDD,[35,36] their efficacy requires several weeks of administration.[35,37] Notably, chronic SSRI administration increases the spontaneous activity of DRN 5-HT neurons and enhances the SSRI-induced increases in extracellular serotonin concentration *in vivo*, *ex vivo*, and *in vitro*.[38–41] However, the causal relationship between the increased DRN 5-HT neuron activity and antidepressant-like effects remains elusive. In this study, we mimicked this increased DRN 5-HT neuron activity after chronic SSRI treatment using optogenetics. Repeated DRN 5-HT and 5-HT$^{DRN\rightarrow VTA}$ neuron activation improved the lack of sociality and the increase in passive coping caused by CSDS, even without extrinsic activation during behavioral analyses. These results indicate that persistent recovery from a depressed state can occur when DRN 5-HT neurons are in a high-activity state, even intermittently. We found that repeated DRN 5-HT neuron stimulation for 5 days was sufficient to reverse CSDS-induced depression-like behaviors, whereas 3–4 weeks of chronic treatment with antidepressants is usually required for a similar effect.[7,42] This apparent discrepancy may be explained by the hypoactivity of DRN 5-HT neurons in susceptible but not resilient mice after CSDS.[6] As most antidepressants affect the serotonin transporters that mediate reuptake of released serotonin, antidepressant effects should depend on the quantity of released serotonin, which depends on 5-HT neuron activity.[43,44] Therefore, DRN 5-HT neuron hypoactivity may attenuate the efficacy of antidepressants, whereas optogenetic activation reliably triggers action potentials, leading to rapid antidepressant-like effects. Supporting this, we reported that ketamine, a rapidly acting antidepressant,[45,46] releases serotonin quickly by activating $\alpha4\beta2$ nicotinic and α-amino-3-hydroxy-5-methyl-4-isoxazolepropionic acid receptors in the DRN.[47,48]

Activation of DRN 5-HT neurons and 5-HT$^{DRN\rightarrow VTA}$ neurons preferentially reactivated the positive dDG ensemble. The exact reason for preferential reactivation is unclear; a recent preprint indicated that engrams that were initially nonselective became selective after memory consolidation.[49] Thus, the memory consolidation process may associate positive emotion induced by various rewards with an ensemble of neurons that were unrelated to positive emotion before the initiation of the experiment. Afterward, stimulation of 5-HT$^{DRN\rightarrow VTA}$ neurons, which rapidly induces positive emotion, as we and others have demonstrated,[30,34] may result in preferential reactivation of neuronal ensembles related to positive emotion. There was no significant difference in the number of tagged neurons after positive, neutral, and negative experiences or in the number of c-fos-positive cells after stimulation of DRN 5-HT neurons. These results imply different downstream circuitry among these ensembles. Ramirez et al. have shown that activation of positive dDG ensembles but not neutral ensembles increased the number of c-fos-positive cells in the nucleus accumbens (NAc) shell and amygdala.[26] Therefore, positive dDG ensembles may preferentially activate neuronal ensembles in these brain regions, which may lead to its long-term antidepressive effect.

We determined that dopaminergic signaling was necessary for the increase in active coping behavior and positive dDG ensembles reactivation elicited by 5-HT$^{DRN\rightarrow VTA}$. Conversely, pharmacological inhibition of dopaminergic signaling did not affect the recovery of social interaction elicited by 5-HT$^{DRN\rightarrow VTA}$. This indicates that active coping with inescapable stress and recovery from a lack of sociality are mediated by discrete neuron types in the VTA, with dopaminergic neurons mediating the former. Phasic activation of VTA dopaminergic neurons provides rapid relief of a depression-like state induced by chronic mild stress,[50] whereas the same stimulation exacerbates a depression-like state induced by CSDS.[51] Although these results are apparently inconsistent, the former study measured active coping behavior in a TST as a proxy for a depressive state while the latter study used lack of sociality induced by CSDS. We found that dopaminergic signaling is central to increasing active coping behavior but not to the recovery of sociality, consistent with the findings of both reports.[50,51] In this context, the pharmacological inhibition of dopaminergic signaling should enhance recovery from a lack of sociality through 5-HT$^{DRN\rightarrow VTA}$ neuron stimulation. However, we did not observe such an enhancement. This apparent discrepancy could be explained partly by a ceiling effect, as the social interaction ratio of mice without CSDS is reported to be approximately 1.5,[52] which is similar to that of the mice subjected to chronic 5-HT$^{DRN\rightarrow VTA}$ neuron stimulation after CSDS

Figure 3. Activation of the DRN 5-HT neurons projecting to the VTA elicits an antidepressant-like effect, and the dDG neuronal ensemble reactivation is preferentially associated with positive experience

(A) Schematic illustration of experiment.

(B) eGFP expression in the VTA (surrounded by a yellow dotted line); scale bar: 100 μm.

(C) Experimental design.

(D) Top: Schematic illustration of the chamber and representative heat maps (target session). Bottom: Time spent in the interaction zone. Social interaction ratio: the ratio of time spent in the interaction zone during a target and no-target session; n = 22 (Venus) and 20 (CheRiff) mice.

(E) Immobility duration in the tail suspension test; n = 22 (Venus) and 21 (CheRiff) mice.

(F) Locomotor activity in the open field test; n = 22 (Venus) and 17 (CheRiff) mice.

(G–I) Quantification of c-fos$^+$mCherry$^+$-to-c-fos$^+$ (G) and -mCherry$^+$ (H) cell colocalization rates, and c-fos$^+$mCherry$^+$ cell numbers (I); n = 6 (CheRiff-Positive), 5 (CheRiff-Negative, Venus-Positive, and Venus-Neutral), and 4 (CheRiff-Neutral and Venus-Negative) mice. $^{**}p < 0.01$, $^{***}p < 0.001$. See also Figure S3.

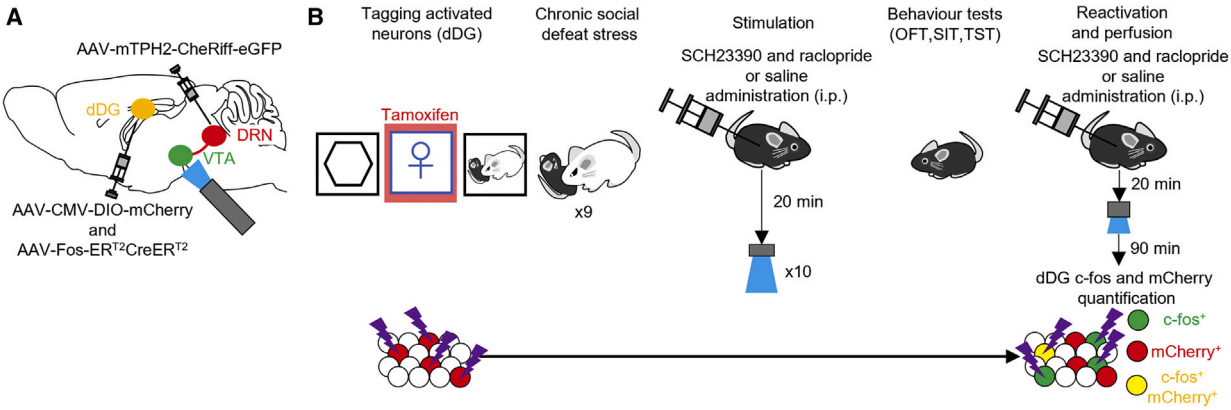

C (Social interaction test)

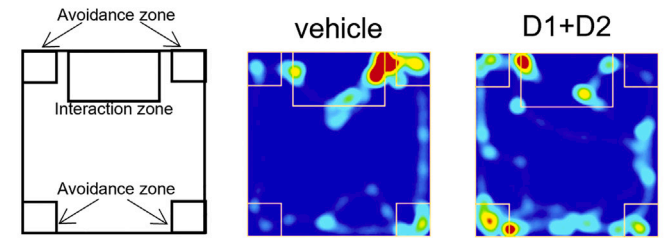

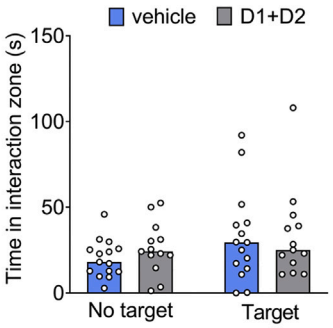

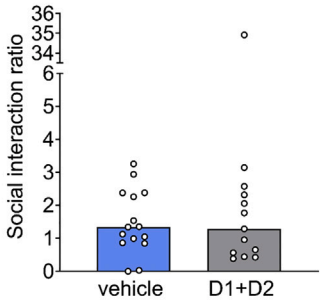

D (Tail suspension test)

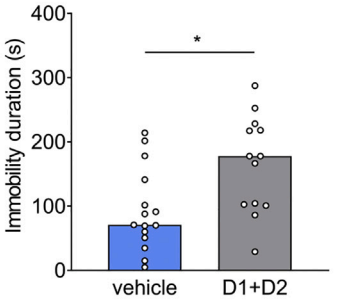

E (Open field test)

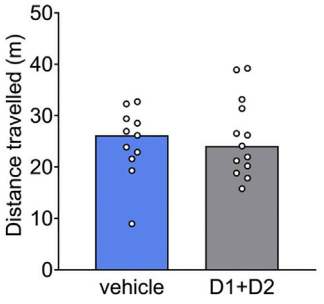

F

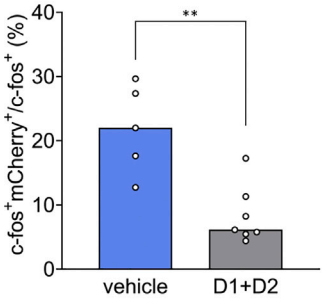

G

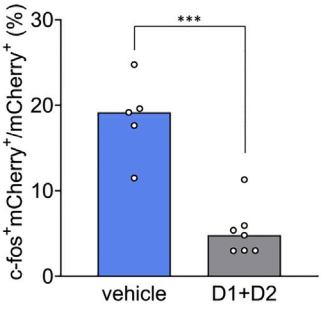

H

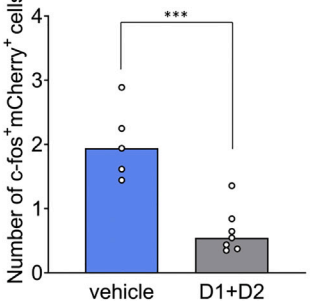

(legend on next page)

(Figure 3D). Systemic injection of a mixture of DA antagonists inhibited the increase in active coping behaviors and the reactivation of positive dDG ensembles in response to 5-HT$^{DRN\rightarrow VTA}$ neurons. The location of the responsible dopaminergic receptors is unclear. A previous report has shown that dopamine receptor blockade in the NAc by intra-NAc injection of dopamine antagonists reduces active coping behavior induced by VTA dopaminergic neurons,[50] indicating the possible involvement of dopamine receptors in the NAc. Because this previous report evaluated the acute effect of dopamine receptor antagonists, further investigation examining the effect of repeated intra-NAc injection of dopamine antagonists will be necessary. Moreover, clinical reports have shown that high heterogeneity exists in the symptom patterns of patients with MDD,[53–55] highlighting the importance of elucidating the biological basis of each MDD symptom. Taken together, our data indicate the critical role of 5-HT$^{DRN\rightarrow VTA}$ neurons and downstream dopaminergic signaling in active coping, a stress response that is often damaged in patients with MDD,[56,57] whereas activation of 5-HT$^{DRN\rightarrow VTA}$ neurons reverses the lack of social reward induced by chronic stress in a dopamine-independent manner.

Limitations of the study

The limitations of the study are twofold: low efficiency of ensemble labeling and lack of analysis for ensembles in other brain regions. In this study, we used a viral-vector-based strategy to target memory ensembles, as in previous reports.[58,59] However, it is difficult and unrealistic to label all neurons that consist of memory ensembles throughout the dDG by this method. Indeed, we found that approximately 70% of c-fos-positive neurons after activation of DRN 5-HT neurons were not labeled by transgenes. This low efficiency also indicates that activation of only part of the positive dDG ensemble was sufficient for an antidepressive effect (Figures 1F–1L). Meanwhile, this also suggests that it is impractical to examine the necessity of positive ensembles for the antidepressive effect of DRN 5-HT neurons through a viral-vector-based method because the activation of some positive ensemble neurons that were not labeled by viral vectors should be sufficient for the antidepressive effect. The utilization of transgenic animals such as Pomc-Cre mice[60] and TRAP2 mice[61] will be necessary to overcome this limitation. Another limitation is that our analysis was restricted to the dDG. Considering that memory-related neuronal ensembles have been found in a number of brain regions, including the medial prefrontal cortex[62] and amygdala,[63,64] positive ensembles in these brain regions may be involved in the antidepressive effect. Because recovery of social reward after chronic stress was not correlated with reactivation of positive dDG ensembles, it is possible that positive ensembles in other brain regions mediate the recovery of social reward due to activation of DRN 5-HT neurons. In particular, a previous report indicated that NAc-projecting mPFC neurons bidirectionally control social interaction behaviors, suggesting a possible role of positive mPFC ensembles.[65]

In summary, we showed that 5-HT$^{DRN\rightarrow VTA}$ neurons preferentially reactivate positive memory ensembles in the dDG. Furthermore, we showed that DA signaling mediates increased active coping behavior and reactivation of a positive memory ensemble in the dDG but not recovery from a lack of sociality through 5-HT$^{DRN\rightarrow VTA}$ neuron activation. Considering the heterogeneity of symptom patterns in patients with MDD, our study provides insights into the biological basis of antidepressant efficacy and could aid the development of drugs that would selectively and effectively mitigate a subset of symptoms in patients with MDD.

STAR★METHODS

Detailed methods are provided in the online version of this paper and include the following:

- KEY RESOURCES TABLE
- RESOURCE AVAILABILITY
  - Lead contact
  - Materials availability
  - Data and code availability
- EXPERIMENTAL MODEL AND SUBJECT DETAILS
  - Animals
  - Experimental design
- METHOD DETAILS
  - Vector construction
  - Production and purification of adeno-associated virus (AAV) vector
  - Stereotaxic surgeries
  - Tagging of dDG ensemble
  - Chronic social defeat stress (CSDS)
  - *In vivo* optogenetic manipulation
  - Optogenetic manipulation with dopamine receptor antagonists
  - Behavioral tests
  - Histological analyses
- QUANTIFICATION AND STATISTICAL ANALYSIS

SUPPLEMENTAL INFORMATION

Supplemental information can be found online at https://doi.org/10.1016/j.celrep.2023.112149.

Figure 4. DA signaling is necessary for increased active coping behavior and preferential reactivation of dDG-positive ensembles but not for the recovery from a lack of sociality elicited by the activation of the 5-HT$^{DRN\rightarrow VTA}$ neurons

(A) Schematic illustration of experiment.

(B) Experimental design.

(C) Top: Schematic illustration of the chamber and representative heat maps (target session). Bottom: Time spent in the interaction zone. Social interaction ratio: the ratio of time spent in the interaction zone during a target and no-target session; n = 15 (vehicle) and 13 (D1+D2) mice.

(D) Immobility duration in the tail suspension test; n = 15 (vehicle) and 13 (D1+D2) mice.

(E) Locomotor activity in the open field test; n = 11 (vehicle) and 13 (D1+D2) mice.

(F–H) Quantification of c-fos$^+$mCherry$^+$-to-c-fos$^+$ (F) and -mCherry$^+$ (G) cell colocalization rates, and c-fos$^+$mCherry$^+$ cell numbers (H); n = 5 (vehicle) and 7 (D1+D2) mice. *p < 0.05, **p < 0.01, ***p < 0.001. See also Figure S4.

ACKNOWLEDGMENTS

We thank Drs. A. Cohen (CheRiff; addgene #51694) and K. Deisseroth (ChETA; addgene #26967) for providing the constructs. We thank Drs. H. Miyoshi and A. Miyawaki (RIKEN, Japan) for providing pCSII-Venus-PRE. This work was supported by JSPS KAKENHI, grant numbers JP20H04774 (K. Nagayasu), JP20K07064 (K. Nagayasu), JP20H03391 (A.K.), JP22K19378 (A.K.), JP19K07121 (H.H.), JP20H00492 (H.H.), JP21K19335 (H.H.), JP18H04616 (S.K.), JP20H00491 (S.K.); MEXT KAKENHI, grant number JP18H05416 (H.H. and T.N.); AMED, grant numbers JP21dm0207117 (H.H.), JP20ak0101088h0003 (S.K.), JP21ak0101153h0001 (S.K.); Platform Project for Supporting Drug Discovery and Life Science Research (BINDS), grant number JP22am0101084 (H.H.); and grants from The Shimizu Foundation for Immunology and Neuroscience (K. Nagayasu), The Uehara Memorial Foundation (K. Nagayasu), the Lotte Research Promotion Grant (K. Nagayasu), and the Takeda Science Foundation (H.H.).

AUTHOR CONTRIBUTIONS

Y.N., K. Nagayasu, and S.K. conceptualized, designed, and supervised all aspects of the study. Y.N., Y.K., K. Nomura, and H.S. performed behavioral experiments. N.N., C.A., M.K., H.K., and K. Nagayasu designed, constructed, and produced AAVs for optogenetic manipulation. K.S., A.K., T.N., and H.H. designed, constructed, and produced AAVs for tagging neuronal ensembles. Y.N., Y.K., and K. Nomura performed histological analyses. Y.N. wrote the manuscript draft. K. Nagayasu and S.K. jointly wrote and finalized the manuscript with inputs from all authors.

DECLARATION OF INTERESTS

The authors declare no competing interests.

Received: August 6, 2022
Revised: November 24, 2022
Accepted: February 6, 2023

REFERENCES

1. Belmaker, R.H., and Agam, G. (2008). Major depressive disorder. N. Engl. J. Med. *358*, 55–68. https://doi.org/10.1056/NEJMra073096.
2. Kupfer, D.J., Frank, E., and Phillips, M.L. (2012). Major depressive disorder: new clinical, neurobiological, and treatment perspectives. Lancet *379*, 1045–1055. https://doi.org/10.1016/S0140-6736(11)60602-8.
3. Zill, P., Baghai, T.C., Zwanzger, P., Schüle, C., Eser, D., Rupprecht, R., Möller, H.J., Bondy, B., and Ackenheil, M. (2004). SNP and haplotype analysis of a novel tryptophan hydroxylase isoform (TPH2) gene provide evidence for association with major depression. Mol. Psychiatr. *9*, 1030–1036. https://doi.org/10.1038/sj.mp.4001525.
4. Zhang, X., Gainetdinov, R.R., Beaulieu, J.M., Sotnikova, T.D., Burch, L.H., Williams, R.B., Schwartz, D.A., Krishnan, K.R.R., and Caron, M.G. (2005). Loss-of-function mutation in tryptophan hydroxylase-2 identified in unipolar major depression. Neuron *45*, 11–16. https://doi.org/10.1016/j.neuron.2004.12.014.
5. Van Den Bogaert, A., Sleegers, K., De Zutter, S., Heyrman, L., Norrback, K.-F., Adolfsson, R., Van Broeckhoven, C., and Del-Favero, J. (2006). Association of brain-specific tryptophan hydroxylase, TPH2, with unipolar and bipolar disorder in a Northern Swedish, isolated population. Arch. Gen. Psychiatr. *63*, 1103–1110. https://doi.org/10.1001/archpsyc.63.10.1103.
6. Challis, C., Boulden, J., Veerakumar, A., Espallergues, J., Vassoler, F.M., Pierce, R.C., Beck, S.G., and Berton, O. (2013). Raphe GABAergic neurons mediate the acquisition of avoidance after social defeat. J. Neurosci. *33*, 13978–13988. https://doi.org/10.1523/JNEUROSCI.2383-13.2013.
7. Sachs, B.D., Ni, J.R., and Caron, M.G. (2015). Brain 5-HT deficiency increases stress vulnerability and impairs antidepressant responses following psychosocial stress. Proc. Natl. Acad. Sci. USA *112*, 2557–2562. https://doi.org/10.1073/pnas.1416866112.
8. Natarajan, R., Forrester, L., Chiaia, N.L., and Yamamoto, B.K. (2017). Chronic-stress-induced behavioral changes associated with subregion-selective serotonin cell death in the dorsal raphe. J. Neurosci. *37*, 6214–6223. https://doi.org/10.1523/JNEUROSCI.3781-16.2017.
9. Byerley, W.F., Reimherr, F.W., Wood, D.R., and Grosser, B.I. (1988). Fluoxetine, a selective serotonin uptake inhibitor, for the treatment of outpatients with major depression. J. Clin. Psychopharmacol. *8*, 112–115.
10. Muijen, M., Roy, D., Silverstone, T., Mehmet, A., and Christie, M. (1988). A comparative clinical trial of and placebo in depressed outpatients. Acta Psychiatr. Scand. *78*, 384–390.
11. Feighner, J.P., and Overø, K. (1999). Multicenter, placebo-controlled, fixed-dose study of citalopram in moderate-to-severe depression. J. Clin. Psychiatr. *60*, 824–830. https://doi.org/10.4088/JCP.v60n1204.
12. Mann, J.J. (1999). Role of the serotonergic system in the pathogenesis of major depression and suicidal behavior. Neuropsychopharmacology *21*, 99–105.
13. Köhler, S., Cierpinsky, K., Kronenberg, G., and Adli, M. (2016). The serotonergic system in the neurobiology of depression: relevance for novel antidepressants. J. Psychopharmacol. *30*, 13–22. https://doi.org/10.1177/0269881115609072.
14. Teissier, A., Chemiakine, A., Inbar, B., Bagchi, S., Ray, R.S., Palmiter, R.D., Dymecki, S.M., Moore, H., and Ansorge, M.S. (2015). Activity of raphé serotonergic neurons controls emotional behaviors. Cell Rep. *13*, 1965–1976. https://doi.org/10.1016/j.celrep.2015.10.061.
15. Ren, J., Friedmann, D., Xiong, J., Liu, C.D., Ferguson, B.R., Weerakkody, T., DeLoach, K.E., Ran, C., Pun, A., Sun, Y., et al. (2018). Anatomically defined and functionally distinct dorsal raphe serotonin sub-systems. Cell *175*, 472–487.e20. https://doi.org/10.1016/j.cell.2018.07.043.
16. Nishitani, N., Nagayasu, K., Asaoka, N., Yamashiro, M., Andoh, C., Nagai, Y., Kinoshita, H., Kawai, H., Shibui, N., Liu, B., et al. (2019). Manipulation of dorsal raphe serotonergic neurons modulates active coping to inescapable stress and anxiety-related behaviors in mice and rats. Neuropsychopharmacology *44*, 721–732. https://doi.org/10.1038/s41386-018-0254-y.
17. Zou, W.-J., Song, Y.-L., Wu, M.-Y., Chen, X.-T., You, Q.-L., Yang, Q., Luo, Z.-Y., Huang, L., Kong, Y., Feng, J., et al. (2020). A discrete serotonergic circuit regulates vulnerability to social stress. Nat. Commun. *11*, 4218. https://doi.org/10.1038/s41467-020-18010-w.
18. Bower, G.H. (1987). Commentary on mood and memory. Behav. Res. Ther. *25*, 443–455. https://doi.org/10.1016/0005-7967(87)90052-0.
19. Gotlib, I.H., Kasch, K.L., Traill, S., Joormann, J., Arnow, B.A., and Johnson, S.L. (2004). Coherence and specificity of information-processing biases in depression and social phobia. J. Abnorm. Psychol. *113*, 386–398. https://doi.org/10.1037/0021-843X.113.3.386.
20. Hamilton, J.P., and Gotlib, I.H. (2008). Neural substrates of increased memory sensitivity for negative stimuli in major depression. Biol. Psychiatr. *63*, 1155–1162. https://doi.org/10.1016/j.biopsych.2007.12.015.
21. Gaddy, M.A., and Ingram, R.E. (2014). A meta-analytic review of mood-congruent implicit memory in depressed mood. Clin. Psychol. Rev. *34*, 402–416. https://doi.org/10.1016/j.cpr.2014.06.001.
22. Sin, N.L., and Lyubomirsky, S. (2009). Enhancing well-being and alleviating depressive symptoms with positive psychology interventions: a practice-friendly meta-analysis. J. Clin. Psychol. *65*, 467–487. https://doi.org/10.1002/jclp.20593.
23. Schacter, D.L., Eich, J.E., and Tulving, E. (1978). Richard Semon's theory of memory. J. Verb. Learn. Verb. Behav. *17*, 721–743. https://doi.org/10.1016/S0022-5371(78)90443-7.
24. Frankland, P.W., Josselyn, S.A., and Köhler, S. (2019). The neurobiological foundation of memory retrieval. Nat. Neurosci. *22*, 1576–1585. https://doi.org/10.1038/s41593-019-0493-1.

25. Josselyn, S.A., and Tonegawa, S. (2020). Memory engrams: recalling the past and imagining the future. Science *367*, eaaw4325. https://doi.org/10.1126/science.aaw4325.

26. Ramirez, S., Liu, X., MacDonald, C.J., Moffa, A., Zhou, J., Redondo, R.L., and Tonegawa, S. (2015). Activating positive memory engrams suppresses depression-like behaviour. Nature *522*, 335–339. https://doi.org/10.1038/nature14514.

27. Zhang, T.R., Larosa, A., Di Raddo, M.E., Wong, V., Wong, A.S., and Wong, T.P. (2019). Negative memory engrams in the hippocampus enhance the susceptibility to chronic social defeat stress. J. Neurosci. *39*, 7576–7590. https://doi.org/10.1523/JNEUROSCI.1958-18.2019.

28. Andoh, C., Nishitani, N., Hashimoto, E., Nagai, Y., Takao, K., Miyakawa, T., Nakagawa, T., Mori, Y., Nagayasu, K., Shirakawa, H., and Kaneko, S. (2019). TRPM2 confers susceptibility to social stress but is essential for behavioral flexibility. Brain Res. *1704*, 68–77. https://doi.org/10.1016/j.brainres.2018.09.031.

29. Hochbaum, D.R., Zhao, Y., Farhi, S.L., Klapoetke, N., Werley, C.A., Kapoor, V., Zou, P., Kralj, J.M., Maclaurin, D., Smedemark-Margulies, N., et al. (2014). All-optical electrophysiology in mammalian neurons using engineered microbial rhodopsins. Nat. Methods *11*, 825–833. https://doi.org/10.1038/nmeth.3000.

30. Nagai, Y., Takayama, K., Nishitani, N., Andoh, C., Koda, M., Shirakawa, H., Nakagawa, T., Nagayasu, K., Yamanaka, A., and Kaneko, S. (2020). The role of dorsal raphe serotonin neurons in the balance between reward and aversion. Int. J. Mol. Sci. *21*, 2160. https://doi.org/10.3390/ijms21062160.

31. Niu, M., Kasai, A., Tanuma, M., Seiriki, K., Igarashi, H., Kuwaki, T., Nagayasu, K., Miyaji, K., Ueno, H., Tanabe, W., et al. (2022). Claustrum mediates bidirectional and reversible control of stress-induced anxiety responses. Sci. Adv. *8*, eabi6375–14. https://doi.org/10.1126/sciadv.abi6375.

32. Gunaydin, L.A., Yizhar, O., Berndt, A., Sohal, V.S., Deisseroth, K., and Hegemann, P. (2010). Ultrafast optogenetic control. Nat. Neurosci. *13*, 387–392. https://doi.org/10.1038/nn.2495.

33. Li, Y., Zhong, W., Wang, D., Feng, Q., Liu, Z., Zhou, J., Jia, C., Hu, F., Zeng, J., Guo, Q., et al. (2016). Serotonin neurons in the dorsal raphe nucleus encode reward signals. Nat. Commun. *7*, 10503. https://doi.org/10.1038/ncomms10503.

34. Wang, H.L., Zhang, S., Qi, J., Wang, H., Cachope, R., Mejias-Aponte, C.A., Gomez, J.A., Mateo-Semidey, G.E., Beaudoin, G.M.J., Paladini, C.A., et al. (2019). Dorsal raphe dual serotonin-glutamate neurons drive reward by establishing excitatory synapses on VTA mesoaccumbens dopamine neurons. Cell Rep. *26*, 1128–1142.e7. https://doi.org/10.1016/j.celrep.2019.01.014.

35. Bezchlibnyk-Butler, K., Aleksic, I., and Kennedy, S.H. (2000). Citalopram - a review of pharmacological and clinical effects. J. Psychiatry Neurosci. *25*, 241–254.

36. Cipriani, A., Furukawa, T.A., Salanti, G., Geddes, J.R., Higgins, J.P., Churchill, R., Watanabe, N., Nakagawa, A., Omori, I.M., McGuire, H., et al. (2009). Comparative efficacy and acceptability of 12 new-generation antidepressants: a multiple-treatments meta-analysis. Lancet *373*, 746–758. https://doi.org/10.1016/S0140-6736(09)60046-5.

37. Quitkin, F.M., McGrath, P.J., Stewart, J.W., Taylor, B.P., and Klein, D.F. (1996). Can the effects of antidepressants be observed in the first two weeks of treatment? Neuropsychopharmacology *15*, 390–394. https://doi.org/10.1016/0893-133X(95)00272-F.

38. Rutter, J.J., Gundlah, C., and Auerbach, S.B. (1994). Increase in extracellular serotonin produced by uptake inhibitors is enhanced after chronic treatment with fluoxetine. Neurosci. Lett. *171*, 183–186. https://doi.org/10.1016/0304-3940(94)90635-1.

39. Gardier, A.M., Malagié, I., Trillat, A.C., Jacquot, C., and Artigas, F. (1996). Role of 5-HT1A autoreceptors in the mechanism of action of serotoninergic antidepressant drugs: recent findings from in vivo microdialysis studies. Fundam. Clin. Pharmacol. *10*, 16–27. https://doi.org/10.1111/j.1472-8206.1996.tb00145.x.dre.

40. Nagayasu, K., Yatani, Y., Kitaichi, M., Kitagawa, Y., Shirakawa, H., Nakagawa, T., and Kaneko, S. (2010). Utility of organotypic raphe slice cultures to investigate the effects of sustained exposure to selective 5-HT reuptake inhibitors on 5-HT release. Br. J. Pharmacol. *161*, 1527–1541. https://doi.org/10.1111/j.1476-5381.2010.00978.x.

41. Asaoka, N., Nishitani, N., Kinoshita, H., Kawai, H., Shibui, N., Nagayasu, K., Shirakawa, H., Nakagawa, T., and Kaneko, S. (2017). Chronic antidepressant potentiates spontaneous activity of dorsal raphe serotonergic neurons by decreasing GABAB receptor-mediated inhibition of L-type calcium channels. Sci. Rep. *7*, 13609. https://doi.org/10.1038/s41598-017-13599-3.

42. Berton, O., McClung, C.A., DiLeone, R.J., Krishnan, V., Renthal, W., Russo, S.J., Graham, D., Tsankova, N.M., Bolanos, C.A., Rios, M., et al. (2006). Essential role of BDNF in the mesolimbic dopamine pathway in social defeat stress. Science *311*, 864–868. https://doi.org/10.1126/science.1120972.

43. Tatsumi, M., Jansen, K., Blakely, R.D., and Richelson, E. (1999). Pharmacological profile of neuroleptics at human monoamine transporters. Eur. J. Pharmacol. *368*, 277–283. https://doi.org/10.1016/S0014-2999(99)00005-9.

44. Sánchez, C., Bergqvist, P.B.F., Brennum, L.T., Gupta, S., Hogg, S., Larsen, A., and Wiborg, O. (2003). Escitalopram, the S-(+)-enantiomer of citalopram, is a selective serotonin reuptake inhibitor with potent effects in animal models predictive of antidepressant and anxiolytic activities. Psychopharmacology (Berl) *167*, 353–362. https://doi.org/10.1007/s00213-002-1364-z.

45. Berman, R.M., Cappiello, A., Anand, A., Oren, D.A., Heninger, G.R., Charney, D.S., and Krystal, J.H. (2000). Antidepressant effects of ketamine in depressed patients. Biol. Psychiatr. *47*, 351–354. https://doi.org/10.1016/S0006-3223(99)00230-9.

46. Zarate, C.A., Singh, J.B., Carlson, P.J., Brutsche, N.E., Ameli, R., Luckenbaugh, D.A., Charney, D.S., and Manji, H.K. (2006). A randomized trial of an N-methyl-D-aspartate antagonist in treatment-resistant major depression. Arch. Gen. Psychiatr. *63*, 856–864. https://doi.org/10.1001/archpsyc.63.8.856.

47. Nishitani, N., Nagayasu, K., Asaoka, N., Yamashiro, M., Shirakawa, H., Nakagawa, T., and Kaneko, S. (2014). Raphe AMPA receptors and nicotinic acetylcholine receptors mediate ketamine-induced serotonin release in the rat prefrontal cortex. Int. J. Neuropsychopharmacol. *17*, 1321–1326. https://doi.org/10.1017/S1461145714000649.

48. Kinoshita, H., Nishitani, N., Nagai, Y., Andoh, C., Asaoka, N., Kawai, H., Shibui, N., Nagayasu, K., Shirakawa, H., Nakagawa, T., and Kaneko, S. (2018). Ketamine-induced prefrontal serotonin release is mediated by cholinergic neurons in the pedunculopontine tegmental nucleus. Int. J. Neuropsychopharmacol. *21*, 305–310. https://doi.org/10.1093/ijnp/pyy007.

49. Tomé, D.F., Zhang, Y., Aida, T., Sadeh, S., Roy, D.S., and Clopath, C. (2022). Dynamic and selective engrams emerge with memory consolidation. Preprint at bioRxiv. https://doi.org/10.1101/2022.03.13.484167.

50. Tye, K.M., Mirzabekov, J.J., Warden, M.R., Ferenczi, E.A., Tsai, H.C., Finkelstein, J., Kim, S.Y., Adhikari, A., Thompson, K.R., Andalman, A.S., et al. (2013). Dopamine neurons modulate neural encoding and expression of depression-related behaviour. Nature *493*, 537–541. https://doi.org/10.1038/nature11740.

51. Chaudhury, D., Walsh, J.J., Friedman, A.K., Juarez, B., Ku, S.M., Koo, J.W., Ferguson, D., Tsai, H.C., Pomeranz, L., Christoffel, D.J., et al. (2013). Rapid regulation of depression-related behaviours by control of midbrain dopamine neurons. Nature *493*, 532–536. https://doi.org/10.1038/nature11713.

52. Golden, S.A., Covington, H.E., Berton, O., and Russo, S.J. (2011). A standardized protocol for repeated social defeat stress in mice. Nat. Protoc. *6*, 1183–1191. https://doi.org/10.1038/nprot.2011.361.

53. Hasler, G., Drevets, W.C., Manji, H.K., and Charney, D.S. (2004). Discovering endophenotypes for major depression. Neuropsychopharmacology *29*, 1765–1781. https://doi.org/10.1038/sj.npp.1300506.

54. Fried, E.I., and Nesse, R.M. (2015). Depression is not a consistent syndrome: an investigation of unique symptom patterns in the STAR*D study. J. Affect. Disord. *172*, 96–102. https://doi.org/10.1016/j.jad.2014.10.010.

55. Nguyen, T.D., Harder, A., Xiong, Y., Kowalec, K., Hägg, S., Cai, N., Kuja-Halkola, R., Dalman, C., Sullivan, P.F., and Lu, Y. (2022). Genetic heterogeneity and subtypes of major depression. Mol. Psychiatr. *27*, 1667–1675. https://doi.org/10.1038/s41380-021-01413-6.

56. Orzechowska, A., Zajączkowska, M., Talarowska, M., and Gałecki, P. (2013). Depression and ways of coping with stress: a preliminary study. Med. Sci. Mon. Int. Med. J. Exp. Clin. Res. *19*, 1050–1056. https://doi.org/10.12659/MSM.889778.

57. Holubova, M., Prasko, J., Ociskova, M., Grambal, A., Slepecky, M., Marackova, M., Kamaradova, D., and Zatkova, M. (2018). Quality of life and coping strategies of outpatients with a depressive disorder in maintenance therapy – a cross-sectional study. Neuropsychiatric Dis. Treat. *14*, 73–82. https://doi.org/10.2147/NDT.S153115.

58. Matos, M.R., Visser, E., Kramvis, I., van der Loo, R.J., Gebuis, T., Zalm, R., Rao-Ruiz, P., Mansvelder, H.D., Smit, A.B., and van den Oever, M.C. (2019). Memory strength gates the involvement of a CREB-dependent cortical fear engram in remote memory. Nat. Commun. *10*, 2315. https://doi.org/10.1038/s41467-019-10266-1.

59. Rafaeli, R., Kreisel, T., Groysman, M., Adamsky, A., and Goshen, I. (2022). Engram stability and maturation during systems consolidation underlies remote memory. Preprint at bioRxiv. https://doi.org/10.1101/2022.07.31.502182.

60. McHugh, T.J., Jones, M.W., Quinn, J.J., Balthasar, N., Coppari, R., Elmquist, J.K., Lowell, B.B., Fanselow, M.S., Wilson, M.A., and Tonegawa, S. (2007). Dentate gyrus NMDA receptors mediate rapid pattern separation in the hippocampal network. Science *317*, 94–99. https://doi.org/10.1126/science.1140263.

61. DeNardo, L.A., Liu, C.D., Allen, W.E., Adams, E.L., Friedmann, D., Fu, L., Guenthner, C.J., Tessier-Lavigne, M., and Luo, L. (2019). Temporal evolution of cortical ensembles promoting remote memory retrieval. Nat. Neurosci. *22*, 460–469. https://doi.org/10.1038/s41593-018-0318-7.

62. Kitamura, T., Ogawa, S.K., Roy, D.S., Okuyama, T., Morrissey, M.D., Smith, L.M., Redondo, R.L., and Tonegawa, S. (2017). Engrams and circuits crucial for systems consolidation of a memory. Science *356*, 73–78. https://doi.org/10.1126/science.aam6808.

63. Nonaka, A., Toyoda, T., Miura, Y., Hitora-Imamura, N., Naka, M., Eguchi, M., Yamaguchi, S., Ikegaya, Y., Matsuki, N., and Nomura, H. (2014). Synaptic plasticity associated with a memory engram in the basolateral amygdala. J. Neurosci. *34*, 9305–9309. https://doi.org/10.1523/JNEUROSCI.4233-13.2014.

64. Terranova, J.I., Yokose, J., Osanai, H., Marks, W.D., Yamamoto, J., Ogawa, S.K., and Kitamura, T. (2022). Hippocampal-amygdala memory circuits govern experience-dependent observational fear. Neuron *110*, 1416–1431.e13. https://doi.org/10.1016/j.neuron.2022.01.019.

65. Murugan, M., Jang, H.J., Park, M., Miller, E.M., Cox, J., Taliaferro, J.P., Parker, N.F., Bhave, V., Hur, H., Liang, Y., et al. (2017). Combined social and spatial coding in a descending projection from the prefrontal cortex. Cell *171*, 1663–1677.e16. https://doi.org/10.1016/j.cell.2017.11.002.

66. Zhang, T., Yanagida, J., Kamii, H., Wada, S., Domoto, M., Sasase, H., Deyama, S., Takarada, T., Hinoi, E., Sakimura, K., et al. (2020). Glutamatergic neurons in the medial prefrontal cortex mediate the formation and retrieval of cocaine-associated memories in mice. Addiction Biol. *25*, e12723. https://doi.org/10.1111/adb.12723.

67. Franklin, K.B.J., and Paxinos, G. (2007). The Mouse Brain in Stereotaxic Coordinates, 3rd edn (Academic Press).

68. Espallergues, J., Teegarden, S.L., Veerakumar, A., Boulden, J., Challis, C., Jochems, J., Chan, M., Petersen, T., Deneris, E., Matthias, P., et al. (2012). HDAC6 regulates glucocorticoid receptor signaling in serotonin pathways with critical impact on stress resilience. J. Neurosci. *32*, 4400–4416. https://doi.org/10.1523/JNEUROSCI.5634-11.2012.

STAR★METHODS

KEY RESOURCES TABLE

REAGENT or RESOURCE	SOURCE	IDENTIFIER
Antibodies		
rabbit polyclonal anti-green fluorescent protein (GFP) antibody	Life Technologies	A-11122; RRID:AB_221569
sheep polyclonal anti-tryptophan hydroxylase (TPH) antibody	Merck Millipore	AB1541; RRID:AB_90754
mouse monoclonal anti-c-fos antibody (2H2)	Novus Biologicals	NBP2-50037; RRID:AB_2665387
rabbit polyclonal anti-DsRed antibody	Takara Bio	632496; RRID:AB_10013483
rabbit polyclonal anti-tyrosine hydroxylase (TH) antibody	Merck Millipore	AB152; RRID:AB_390204
Alexa Fluor 488-labeled donkey anti-rabbit IgG	Thermo Fisher Scientific	A-21206; RRID:AB_2535792
Alexa Fluor 594-labeled donkey anti-rabbit IgG	Thermo Fisher Scientific	A-21207; RRID:AB_141637
Alexa Fluor 594-labeled donkey anti-sheep IgG	Thermo Fisher Scientific	A-11016; RRID:AB_2534083
Alexa Fluor 488-labeled donkey anti-mouse IgG	Thermo Fisher Scientific	A-21202; RRID:AB_141607
Alexa Fluor 594-labeled donkey anti-mouse IgG	Thermo Fisher Scientific	A-21203; RRID:AB_141633
Chemicals, peptides, and recombinant proteins		
Tamoxifen	Toronto Research Chemicals	T006000
SCH23390	Sigma-Aldrich	D054
Raclopride	Abcam	ab120563
Experimental models: Cell lines		
Lenti-X 293T	Clontech	632180
Experimental models: Organisms/strains		
C57BL/6J mice	Japan SLC	RRID: IMSR_JAX:000,664
Recombinant DNA		
AAV-mTPH2-CheRiff-eGFP	in house	PMID: 32245184 (Nagai et al.[30])
AAV-mTPH2-Venus	in house	PMID: 32245184 (Nagai et al.[30])
AAV-Fos-ER^{T2}CreER^{T2}	in house	PMID: 35302853 (Niu et al.[31])
AAV-CMV-DIO-ChETA-eYFP	in house	in this study
AAV-CMV-DIO-mCherry	in house	in this study

RESOURCE AVAILABILITY

Lead contact

Further information and requests for data, resources, and reagents should be directed to and will be fulfilled by the lead contact Kazuki Nagayasu (nagayasu@pharm.kyoto-u.ac.jp).

Materials availability

Plasmids generated in this study will be made available on request to the lead contact.

Data and code availability

- All data reported in this paper will be shared by the lead contact upon request.
- This paper does not report original code.
- Any additional information required to reanalyze the data reported in this work paper is available from the lead contact upon request.

EXPERIMENTAL MODEL AND SUBJECT DETAILS

Animals

All mice were handled in accordance with the ethical guidelines of the Kyoto University Animal Research Committee (approval code: 13-41-2, 19-41-1,2,3). Adult male C57BL/6J mice (8–12 weeks old, Japan SLC, Shizuoka, Japan) were housed in groups (no more than six mice in an individual cage) with free access to food and water, and kept under constant ambient temperature (24 ± 1°C) and humidity (55 ± 10%), with a 12 h light-dark cycles. Mice were randomly assigned to each experimental group.

Experimental design

The time course of behavioral experiments in detail was described in Figures S1A, S1B, S3A, and S4A. A cohort of mice were injected with AAV-mTPH2-Venus or AAV-mTPH2-CheRiff-eGFP into the DRN and AAV-Fos-ER^{T2}CreER^{T2} together with AAV-CMV-DIO-mCherry into the dDG. Four weeks later, fiber optic cannula was implanted to the DRN. Tamoxifen (3 mg/mouse, i.p.[31]) was administered 6 h before cohabitation with a female mouse (positive experience), exploration in a novel cage (neutral experience), or single session of social defeat (negative experience). Three (CheRiff) and six (Venus) mice were not administered with AAV-Fos-ER^{T2}CreER^{T2} and AAV-CMV-DIO-mCherry. These mice were not administered with tamoxifen and were not subjected to positive and neutral experiences but subjected to ten sessions of social defeat. Other mice were subjected to one positive experience, one neutral experience, and one negative experience regardless of the type of tagged ensembles. Afterward, nine sessions of social defeat were applied, so that all mice were defeated ten times according to the previous reports.[28,52] After social defeat, mice underwent optogenetic stimulation, open field test, social interaction test and tail suspension test (Figures 1A–1E). Thereafter, these mice received optogenetic activation of DRN 5-HT neurons and perfused 90 min later. The number of c-fos$^+$, mCherry$^+$, c-fos$^+$mCherry$^+$, and DAPI$^+$ cells in the dDG were counted by immunohistochemistry (Figure 2). Another cohort of mice were injected with AAV-Fos-ER^{T2}CreER^{T2} together with AAV-CMV-DIO-mCherry or AAV-CMV-DIO-ChETA-eYFP into the dDG, and 4 weeks after, they received an implantation of the fiber optic cannula into the dDG. Following tagging of dDG positive ensemble with mCherry, mice underwent CSDS, chronic stimulation of dDG positive ensemble, open field test, social interaction test and tail suspension test (Figures 1F–1L). Thereafter, these mice received the reactivation of dDG positive ensemble and were perfused 90 min later. The number of c-fos$^+$, TPH2$^+$, c-fos$^+$TPH2$^+$, or DAPI$^+$ cells in the DRN were counted by immunohistochemistry (Figures S2D–S2I). Another cohort of mice were injected with AAV-mTPH2-Venus or AAV-mTPH2-CheRiff-eGFP into the DRN and AAV-Fos-ER^{T2}CreER^{T2} together with AAV-CMV-DIO-mCherry into the dDG. Four weeks later, they received an implantation of fiber optic cannula into the VTA. Following tagging dDG ensemble with mCherry, mice underwent CSDS, chronic stimulation of 5-HT$^{DRN\rightarrow VTA}$ neuron, open field test, social interaction test, and tail suspension test (Figures 3A–3F). Thereafter, these mice received activation of 5-HT$^{DRN\rightarrow VTA}$ neuron and were perfused 90 min later. The number of c-fos$^+$, mCherry$^+$, c-fos$^+$mCherry$^+$, or DAPI$^+$ cells in the dDG were counted by immunohistochemistry (Figures 3G–3I). Another cohort of mice were injected with AAV-mTPH2-CheRiff-eGFP into the DRN and AAV-Fos-ER^{T2}CreER^{T2} together with AAV-CMV-DIO-mCherry into the dDG. Four weeks later, they received an implantation of the fiber optic cannula into the VTA. Following tagging of dDG positive ensemble with mCherry, mice underwent CSDS, chronic stimulation of 5-HT$^{DRN\rightarrow VTA}$ neurons with pretreatment with SCH23390 and raclopride 20 min before the optogenetic stimulation. Further, mice underwent open field test, social interaction test, and tail suspension test (Figures 4A–4E). Thereafter, these mice received reactivation of 5-HT$^{DRN\rightarrow VTA}$ neuron with pretreatment with SCH23390 and raclopride 20 min before the optogenetic stimulation, and were perfused 90 min later. The number of c-fos$^+$, mCherry$^+$, c-fos$^+$mCherry$^+$, or DAPI$^+$ cells in the dDG were counted by immunohistochemistry (Figures 4F–4H). As a control, another cohort of mice were injected with AAV-mTPH2-CheRiff-eGFP into the DRN and AAV-Fos-ER^{T2}CreER^{T2} together with AAV-CMV-DIO-mCherry into the dDG. This cohort of mice were subjected to tagging of positive ensembles and CSDS but not to chronic stimulation of 5-HT$^{DRN\rightarrow VTA}$ neurons. Instead of photoactivation, mice were administered with SCH23390 and raclopride similar to above mentioned cohort. Further, mice underwent open field test, social interaction test, and tail suspension test (Figure S4F). Thereafter, these mice were treated with SCH23390 and raclopride and were perfused 110 (= 20 + 90) minutes later. The number of c-fos$^+$, mCherry$^+$, or c-fos$^+$mCherry$^+$ cells in the dDG were counted by immunohistochemistry (Figure S4G). As a further control in tail suspension test, another cohort of mice were injected with AAV-mTPH2-Venus into the DRN and AAV-Fos-ER^{T2}CreER^{T2} together with AAV-CMV-DIO-mCherry into the dDG. This cohort of mice were subjected to tagging of positive ensembles, CSDS, and chronic stimulation of 5-HT$^{DRN\rightarrow VTA}$ neurons with pretreatment with SCH23390 and raclopride 20 min before the optogenetic stimulation. Further, mice underwent tail suspension test (Figure S4H).

METHOD DETAILS

Vector construction

For construction of AAV-CMV-DIO-ChETA-eYFP, ChETA-eYFP fragment and CMV promoter was amplified by PCR from pTYF-smTPH2-ChETA-eYFP[16] and pFUW-CMV-DIO-Magneto2.0-sNRPpA (Addgene, 74,307), respectively. Fragments were ligated to the AAV backbone obtained from pAAV-hSyn-DIO-hM3Dq-mCherry (Addgene, 44,361). For construction of AAV-CMV-DIO-mCherry, the CMV promoter fragment amplified by PCR from pFUW-CMV-DIO-Magneto2.0-sNRPpA (Addgene, 74,307) was ligated to the AAV backbone obtained from pAAV-hSyn-DIO-mCherry.[66] Other plasmids were reported previously.[30,31]

Production and purification of adeno-associated virus (AAV) vector

AAVs were prepared according to the previous report.[30] Lenti-X 293T cells (Clontech, Mountain View, CA, USA) were grown to 60–70% confluency, and 8 μg of pHelper, 5 μg of pAAV-DJ and 5 μg of transfer plasmid were transfected with polyethylenimine (Polysciences, Warrington, PA, USA). After 60–72 h, supernatant was aspirated and the cells were harvested in 500 μL of Gradient Buffer. Four freeze-and-thaw cycles were used to disrupt cell membrane. After addition of 0.5 μL benzonase (Sigma-Aldrich, St. Louis, USA), cell suspension was incubated at 37°C for 45 min and centrifuged for 15 min at 3,000 × g. The supernatant was collected and ultracentrifuged in discontinuous iodixanol density gradient at 48,000 rpm, 18°C for 1 h in 50.4Ti rotor (Beckman-Coulter, Brea, CA, USA). After ultracentrifugation, syringe with an 18-gauge needle was inserted approximately 1–2 mm below the boundary surface between 40% and 58% gradient buffer layers, and slowly extracted solution. They were aliquoted and stored at −80°C. The titer of AAV was measured by qPCR and estimated to be about 1.0×10^{13} IU/mL.

Stereotaxic surgeries

Stereotaxic surgeries were conducted using a small animal stereotaxic frame (Narishige, Tokyo, Japan) according to the Brain Atlas.[67] Mice were anesthetized with sodium pentobarbital (50 mg/kg, i.p., Kyoritsu Seiyaku, Tokyo, Japan) or 3% isofluran (Escain, Pfizer, Tokyo, Japan). AAV-mTPH2-Venus and AAV-mTPH2-CheRiff-eGFP were microinjected at 1 μL into the mouse DRN (anteroposterior (AP) −4.3 mm, mediolateral (ML) 0 mm, dorsoventral (DV) +3.4 mm from the bregma, 20°). 0.4 μL of AAV-Fos-ER^{T2}CreER^{T2} together with AAV-CMV-DIO-mCherry or AAV-CMV-DIO-ChETA-eYFP in a 1:1 ratio was microinjected into the dDG (AP −1.8 mm, ML ±0.8 mm, DV +2.2 mm from the bregma). For optical stimulation, 4 weeks after the viral injection the mice were implanted with a fiber optic cannula so that the tip of the cannula was placed just above the dorsal border of the target regions. The following coordinates (in mm) were used for fiber implant, DRN (AP -4.3 mm, ML +1.2 mm from the bregma, depth +3.3 mm from the skull at 20°), bilateral VTA (AP -3.4 mm, ML ±0.5 mm, DV +4.3 mm from the bregma), bilateral dDG (AP -1.8 mm, ML ±0.8 mm, DV +2.0 mm from the bregma). Mice were individually housed for at least 7 days to recover before tagging activated neurons in dDG and were kept in the singly housed until sacrifice.

Tagging of dDG ensemble

Six hours after tamoxifen administration (TAM; 3 mg/mouse, T006000, Toronto Research Chemicals, Toronto, Canada), mice underwent positive (exposure to a female mouse), neutral (exploration of new cage), or negative (a single social defeat stress) experience. Positive experience: one female mouse (postnatal day 30–40) was introduced into the home cage of experimental male mouse with a clear cage top and the male mice were allowed to interact with a female mouse freely for 2 h. Neutral experience: experimental male mice were placed into a new plastic cage with a clear cage top for 2 h. Negative experience: a single social defeat session. Mice were randomly assigned to one of the three groups.

Chronic social defeat stress (CSDS)

Chronic social defeat stress (CSDS) was applied as described previously.[28] Briefly, male ICR mice were screened based on their aggressiveness to a naive C57BL/6 mouse, as measured by the latency and the number of attacks, and were used as aggressor mice for CSDS. For social defeat stress, the isolated mouse to be defeated was introduced and kept in the home-cage of a resident aggressor ICR mouse for 5 min daily. All mice were exposed to social defeat stress for 10 consecutive days. The pair of defeated and aggressor mice was changed daily to minimize the variability in the aggressiveness of ICR mice. The social interaction test was performed after optical activation as described below.

In vivo optogenetic manipulation

Fiber optic cannulae made of multimode LC/PC ceramic ferrules (1.25 mm outer diameter, 270 μm hole size, Thorlabs, Newton, NJ, USA) and plastic optic fiber (CK10, 250 μm diameter, NA 0.5, Mitsubishi Rayon, Tokyo, Japan). Implanted fiber optic cannula was connected to the fiber-optic patch cord (M83L01, Thorlabs, Newton, NJ, USA) or bifurcated fiber bundle (BFYL2LF01, Thorlabs, Newton, NJ, USA) coupled with the rotary joint (Doric Lenses, QC, Canada). Light emitted from the diode-pumped solid-state (DPSS) laser (Beijing Viasho Technology, Beijing, China) was converged to the fiber optic which was connected to the rotary joint. The DPSS laser was driven by the microcontroller (Arduino SRL, Italy) to generate the pulse width modulation signal. For AAV-mTPH2-Venus and AAV-mTPH2-CheRiff-eGFP mice, after CSDS for 10 consecutive days, blue light illumination for 5 min was delivered twice a day for 5 days (473 nm, 5 mW at the tip of the fiber, 10 ms duration, 20 Hz frequency, 20 s ON/10 s OFF). For AAV-Fos-ER^{T2}CreER^{T2} and AAV-CMV-DIO-mCherry or AAV-CMV-DIO-ChETA-eYFP mice, blue light illumination for 15 min was delivered twice a day for 5 days (473 nm, 10 mW at the tip of the fiber, 15 ms duration, 20 Hz frequency). One day after the final optical activation, mice underwent behavior tests.

Optogenetic manipulation with dopamine receptor antagonists

D1 receptor antagonist SCH23390 (0.1 mg/kg) (Sigma-Aldrich) and D2 receptor antagonist raclopride (2 mg/kg) (ab120563, abcam, Cambridge, UK) was dissolved in saline containing 0.5% dimethyl sulfoxide (DMSO). For optogenetic activation with pharmacological intervention, vehicle (0.5% DMSO in saline) or drugs in a volume equal to 1% of the mouse body weight were administered intraperitoneally 20 min before the optogenetic stimulation (473 nm, 5 mW at the tip of the fiber, 10 ms duration, 20 Hz frequency,

20 s ON/10 s OFF for 5 min). This session was performed twice a day for 5 days. One day after the final optogenetic activation, all mice underwent behavior tests.

Behavioral tests

Open field test

Open field test was performed as described previously.[16] In brief, the open field arena (a white acrylic cube (50 × 50 × 50 cm)) was used to measure locomotor activity. Each animal placed individually into the center of the arena and permitted free exploration. The behavior of the animal was recorded with a camera over a 10 min. The recorded data were analyzed automatically using video tracking system (ANY-maze version 4.99, Stoelting, Wood Dale, IL, USA). Total distance traveled during a session were measured.

Social interaction test

Social interaction test was performed according to previous report.[28] Mice were kept for 150 s in an open field chamber (50 × 50 × 50 cm) with an empty wire mesh cage (10 × 6.5 cm) located at one end of the chamber (no-target session). Consecutively, the same mouse was kept for 150 s in the same open field chamber with an ICR mouse enclosed in the wire mesh cage (target session). Mouse behaviors were video monitored, and the trajectory of mouse ambulation was determined and recorded by ANY-MAZE (Stoelting Co., Wood Dale, IL, USA). The four corners of the chamber (9 cm square) and the area surrounding the wire mesh cage (14 × 24 cm) was defined as the avoidance zone and the interaction zone, respectively. Time spent in the interaction zone during each session were measured. Social interaction ratio was calculated as time spent in the interaction zone in target session divided by that in no-target session.

Tail suspension test

Tail suspension test was performed as described previously.[16] Briefly, the mice were hung on a hook (35 cm from the floor of the test box) with the tail taped to a force-transducer (PowerLab 2/26, AD Instruments, Dunedin, New Zealand) fixed to the ceiling of the test box (40 × 40 × 40 cm). The immobility time was recorded for 6 min.

Histological analyses

After behavioral tests, all mice received a single optogenetic activation. Mice injected with AAV-mTPH2-Venus and AAV-mTPH2-CheRiff-eGFP received blue light stimulation for 5 min (473 nm, 5 mW at the tip of the fiber, 10 ms duration, 20 Hz frequency, 20 s ON/10 s OFF). Mice injected with AAV-Fos-ER^{T2}CreER^{T2} and AAV-CMV-DIO-mCherry or AAV-CMV-DIO-ChETA-eYFP received blue light stimulation for 15 min (473 nm, 10 mW at the tip of the fiber, 15 ms duration, 20 Hz frequency, 20 s ON/10 s OFF). In Figure 4, 20 min after injection of SCH23390 and raclopride or vehicle, mice injected with AAV-mTPH2-CheRiff-eGFP received blue light stimulation for 5 min (473 nm, 5 mW at the tip of the fiber, 10 ms duration, 20 Hz frequency, 20 s ON/10 s OFF). Ninety min after stimulation, all mice were deeply anesthetized under sodium pentobarbital (50 mg/kg) or mixture of medetomidine (0.3 mg/kg) (Kyoritsu Seiyaku, Tokyo, Japan), midazolam (4.0 mg/kg) (FujiPharma, Tokyo, Japan), and butorphanol (5.0 mg/kg) (Meiji Seika Pharma, Tokyo, Japan). Mice were transcardially perfused with phosphate buffer saline (PBS) followed by 4% paraformaldehyde (Nacalai Tesque, Kyoto, Japan) in phosphate buffer. After perfusion fixation, the brains were removed, equilibrated in 15% sucrose in PBS for overnight, and frozen. The brains were cryosectioned into 30 μm-thick coronal sections with the cryostat (Leica CM3050S; Leica Biosystems, Nussloch, Germany) and stored at −20°C until immunohistochemical processing. For immunohistochemistry, the sections including DRN, VTA or dDG were immersed in 0.25% Triton X-100 (Nacalai Tesque) for permeabilization and then incubated overnight at 4°C with rabbit polyclonal anti-green fluorescent protein (GFP) antibody (1:2000; A-11122, Life Technologies, Carlsbad, CA, USA), sheep polyclonal anti-tryptophan hydroxylase (TPH) antibody (1:200; AB1541, Merck Millipore, MA, USA), mouse monoclonal anti-c-fos antibody (2H2) (1:1000, NBP2-50037, Novus Biologicals, CO, USA), rabbit polyclonal anti-DsRed antibody (1:500, 632,496, Takara Bio, Shiga, Japan) and rabbit polyclonal anti-tyrosine hydroxylase (TH) antibody (1:200; AB152, Merck Millipore) followed by incubation with Alexa Fluor 488-labeled donkey anti-rabbit IgG (1:200; A-21206, Thermo Fisher Scientific, MA, USA), Alexa Fluor 594-labeled donkey anti-rabbit IgG (1:200; A-21207, Thermo Fisher Scientific), Alexa Fluor 594-labeled donkey anti-sheep IgG (1:200; A-11016, Thermo Fisher Scientific), Alexa Fluor 488-labeled donkey anti-mouse IgG (1:200; A-21202, Thermo Fisher Scientific) or Alexa Fluor 594-labeled donkey anti-mouse IgG (1:200; A-21203, Thermo Fisher Scientific) for 2 h at room temperature. The sections were then washed in PBS and mounted on glass with Fluoromount/Plus (K048, Diagnostic Biosystems, Pleasanton, CA, USA) or DAPI Fluoromount-G (0100–20, Southern Biotech, Birmingham, AL, USA). Immunofluorescence was visualized using a laser scanning confocal microscopy (Fluoview FV10i, Olympus, Tokyo, Japan). Images were processed with FV10i-SW software (Olympus) and ImageJ software (National Institutes of Health, Bethesda, MD, USA). The number of c-fos, mCherry, GFP, TH and TPH2 positive cells were quantified in at least three different sections and averaged across sections. All AAVs infection and fiber implantation site were verified immunohistochemically. The data points obtained from the mice with failed AAV infection or fiber implantation were excluded. The numbers of the animals used were determined according to the previous reports.[26,27,68]

QUANTIFICATION AND STATISTICAL ANALYSIS

The data are plotted as dots, unless otherwise stated. The bar graph represents median. Statistical analysis was performed by GraphPad Prism (version 8 and 9, GraphPad Software Inc., La Jolla, CA, USA). Two-sided unpaired Student's *t*-test was used for comparisons of 2 individual groups unless otherwise stated. For comparison of social interaction ratio, Mann-Whitney test was used. For comparisons of 3 or more groups, data were compared using two-way analyses of variance (ANOVA), followed by Tukey's multiple comparisons test or two-way repeated measures ANOVA followed by the Sidak's multiple comparisons test. In all cases, p values less than 0.05 ($p < 0.05$) were considered statistically significant.